Interfacial diffusion aided deformation during nanoindentation

Amit Samanta and Weinan E'

Citation: AIP Advances **6**, 075002 (2016); doi: 10.1063/1.4958299
View online: http://dx.doi.org/10.1063/1.4958299
View Table of Contents: http://aip.scitation.org/toc/adv/6/7
Published by the American Institute of Physics

Interfacial diffusion aided deformation during nanoindentation

Amit Samanta[1] and Weinan E[2,a]
[1]*Physics Division, Lawrence Livermore National Laboratory, Livermore, California 94550, USA*
[2]*BICMR and School of Mathematical Sciences, Peking University, Beijing, China and Department of Mathematics and Program in Applied and Computational Mathematics, Princeton University, Princeton, New Jersey 08544, USA*

(Received 29 February 2016; accepted 23 June 2016; published online 6 July 2016)

Nanoindentation is commonly used to quantify the mechanical response of material surfaces. Despite its widespread use, a detailed understanding of the deformation mechanisms responsible for plasticity during these experiments has remained elusive. Nanoindentation measurements often show stress values close to a material's ideal strength which suggests that dislocation nucleation and subsequent dislocation activity dominates the deformation. However, low strain-rate exponents and small activation volumes have also been reported which indicates high temperature sensitivity of the deformation processes. Using an order parameter aided temperature accelerated sampling technique called adiabatic free energy dynamics [J. B. Abrams and M. E. Tuckerman, *J. Phys. Chem. B*, **112**, 15742 (2008)], and molecular dynamics we have probed the diffusive mode of deformation during nanoindentation. Localized processes such as surface vacancy and ad-atom pair formation, vacancy diffusion are found to play an important role during indentation. Our analysis suggests a change in the dominant deformation mode from dislocation mediated plasticity to diffusional flow at high temperatures, slow indentation rates and small indenter tip radii. [http://dx.doi.org/10.1063/1.4958299]

Nanoindentation is a valuable hardness test that provides both a high level of accuracy due to the precision of the indenter tip and improved lateral resolution compared to microindentation. Although it has been extensively used to measure macroscopic properties such as Young's modulus and Poisson's ration, the microscopic mechanisms responsible for plastic deformation during nanoindentation have yet to be elucidated. These mechanisms have been called into question as the small strain rate exponents reported from nanoindentation experiments suggests that deformation is perhaps dominated by diffusive processes, but also the high strength measurements indicates that dislocation mediated processes are dominant.[1–3] Thus, it is important that a detailed understanding is developed regarding these deformation modes to reconcile conflicting observations and to provide a consistent framework for the interpretation of nanoindentation experiments.

The initial load-displacement response from a typical nanoindentation experiment fits well with the Hertzian elasticity theory. As the indentation load increases, however, there is a measurable deflection from this elastic behavior at a critical tip displacement.[4–6] It is widely believed that this deflection, also called the first pop-in, corresponds to the initiation of plasticity through dislocation nucleation in a "dislocation starved" region below the indenter and is followed by deformation through dislocation activity.[5–7] This dislocation dominated picture of plasticity is also supported by indentation simulations.[6,8] However, there is experimental evidence that points to the existence of a diffusive regime during nanoindentation. For example, Wang *et al*. and Schuh *et al*. separately reported activation volumes ($\hat{\Omega}$) of about $0.50b^3$, where b is the Burgers vector, during the initial

[a]Electronic address: weinan@math.princeton.edu

stages of nanoindentation.[2,9,10] This $\hat{\Omega}$ is much smaller than 100-1000b^3, which corresponds to forest hardening[11] that has been observed during microindentation experiments,[12–15] and 1-10b^3 which has been reported for dislocation nucleation.[16,17] It therefore remains unclear how the dislocation dominated deformation picture obtained from most indentation simulations reconciles with these low activation volumes reported from experiments. In this letter, we describe atomistic simulations, with copper as a prototypical material, which were used to analyze the previously unexplored possibility of diffusional flow during nanoindentation.

Until recently, it has been difficult to probe the microscopic deformation mechanisms of macroscopic systems over experimentally relevant time-scales. Laboratory experiments are often limited by spatio-temporal resolution and atomistic simulation tools like molecular dynamics (MD) fail to capture atomic processes with waiting times greater than a few tens of nanoseconds. We were able to overcome the time-scale restriction of MD and bridge the gap between the experimental and simulation time-scales using two methodologies. First, we used an order parameter aided temperature accelerated free energy[18] sampling technique called driven adiabatic free energy dynamics (d-AFED).[19–21] Next, we used high temperatures to accelerate the kinetics of thermally activated processes in MD simulations. Using d-AFED, we were able to investigate the free energy landscape of the system and relevant parts of the configuration space and using high temperature MD, we were able to gain a quantitative understanding of the diffusive processes. From these studies, a clear picture of the diffusive processes emerges: we find that surface vacancy and ad-atom pair formation along with vacancy diffusion play a dominant role during the early stages of indentation.

The central theme of d-AFED is to define a set of order parameters (which we call collective variables) that can capture the interesting transition events taking place in the system. We used the Steinhardt orientation order parameters as collective variables (CVs).[22] Once identified, these CVs can be used to drive the system to systematically and efficiently explore the underlying free energy landscape by exploiting the adiabatic time scale separation between the evolution of the macroscopic variables (i.e. the CVs) and microscopic system (i.e. the atoms). In practice, this time-scale separation is achieved by assigning fictitious masses to the macroscopic variables that are greater than the atomic masses and evolving the macroscopic variables at a temperature that is much higher than the physical temperature. The high temperature assigned to the macroscopic variables ensures that the system can overcome all barriers and explore processes with long waiting times.[19–21]

Because the dynamics of the macroscopic variables in d-AFED are fictitious, important information about the kinetics of the diffusive processes are essentially lost.[19,20] Consequently, we used high temperature MD simulations to gain quantitative insights into these processes. High temperatures provide enough kinetic energy to the system so that it can easily hop from one local minimum to another that allows us to analyze the defect kinetics and determine the parameters that control the transition between the different deformation modes. It is important to note that even though the temperatures used in our simulations are much higher than what is typically used during nanoindentation experiments, they allow us to probe mechanisms that have not been investigated in silico.

We first consider a classical MD indentation simulation performed at 20 K with a spherical indenter of radius 20 Å and an indentation rate of 80 Å/ns.[23] It should be noted that the limited length of MD simulations necessitates the use of indentation rates that are orders of magnitude greater than those typical used in experiments. During this initial indentation simulation, the sample was seen to elastically deform up to a depth of $h \sim 4.20$ Å that was followed by the nucleation of dislocations and extensive dislocation activity. To gain insights into the thermally activated atomic processes whose waiting time is much longer than the time scales accessible in MD, we resorted to d-AFED simulations. We extracted structures from these MD trajectories at indentation depths of $h = 5$ and 15 Å and thermalized them at 300 K while keeping the indenter fixed. Subsequently, multiple d-AFED trajectories were launched from these configurations, keeping the atoms at 300 K and the macroscopic variables at 2×10^7 K.[23] Fig. 1 shows representative snapshots of the indented surface along a d-AFED trajectory. In contrast to the commonly observed high dislocation activity in traditional MD simulations, ad-atom islands were observed in the vicinity of the indenter-sample interface. As the simulation progresses, the population of such islands increases and the islands begin to agglomerate. This is followed by the formation of a continuous band of ad-atoms around

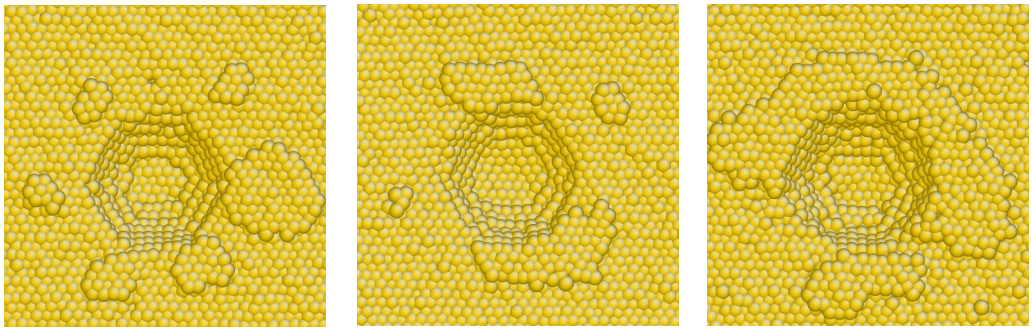

FIG. 1. Snapshots (a) to (c) show the slow evolution of the surface morphology in a AFED sampling trajectory. The atoms are maintained at 300 K, and the indenter is held fixed at $h = 15$ Å. As the simulation progresses, the size of the ad-atom islands along the periphery of the indented region increases and the dislocation density below the indented region decreases.

the indented region. Intuitively, it might be expected that the width of this band of ad-atoms would increase as the d-AFED simulation progresses. However, we find that after the band reaches a critical width, a second layer of ad-atoms islands starts to form on top of the previous layer. It is important to note that this process is observed in all of the d-AFED trajectories which leads us to believe that these processes may play an important part in room temperature experiments. Below the surface, we observe a slow reduction in dislocation density and, simultaneously, atomic rearrangement along the indenter-sample interface. The deformation picture that emerges from these d-AFED simulations is clearly very different from the dislocation-dominated deformation usually captured in MD simulations.

After examining these deformation processes using d-AFED, we investigated their temperature and rate dependencies using classical MD at elevated temperatures. The effect of temperature on the 'pop-in' of the indenter is shown in Fig. S1.[23] The initial part of the load (P) vs indentation depth (h) curve at 20 K matches well with the Hertzian elasticity theory and the sample (initially free of defects) is elastically deformed. After the initial dislocation nucleation at $h \sim 4.20$ Å, we observe intermittent dislocation burst events followed by dislocation propagation and multiplication leading to an increase in the dislocation density.[24–26] Due to extensive shearing, steps are formed on the surface due to dislocation slip on different (111) planes. This can been seen on the sides of the indentation pit in Fig. 2(a). Fig. 2(c) shows the dislocation structures in the indented region below the surface.

In MD simulations performed above 700 K, we observed localized atomic reorganization in the indented regions of the sample where the indenter-sample interface developed (111)-type symmetry. Interestingly, such local atomic reorganizations have been reported from indentation experiments performed under room temperature conditions but never observed in simulations.[27] In the indentation simulations performed at temperatures above 1000 K, we observe extensive healing of the sheared regions of the sample and ad-atom island formation on the surface near the indented region. As h increased, more ad-atoms were formed which coalesced to form islands. These islands then agglomerated to form a continuous band of ad-atoms, similar to what was seen in the d-AFED simulations. The top view of such a surface, indented at 1100 K, is shown in Fig. 2(b). It can be seen in Fig. 2(d) that the diffusive processes activated at high temperatures lead to a significant decrease in dislocation density below the indented region compared to the configurations generated at 20 K (Fig. 2(c)). The absence of dislocation structures during deformation at 1100 K clearly points to the role of point defects in healing the system. Since the diffusive processes relax the high compressive stress field beneath the indenter, it is possible that due to this decrease in the stress, the system is further able to minimize its energy by decreasing the dislocation density. We find that at 1200 K, the deformation mechanism (see Fig. S2)[23] is completely dominated by diffusive processes. The remarkable similarity in the atomic processes observed in d-AFED simulations, in which atoms are maintained at room temperatures, and in the high temperature indentation simulations suggests that these diffusive processes can indeed take place over time-scales relevant to nanoindentation experiments at room temperature.

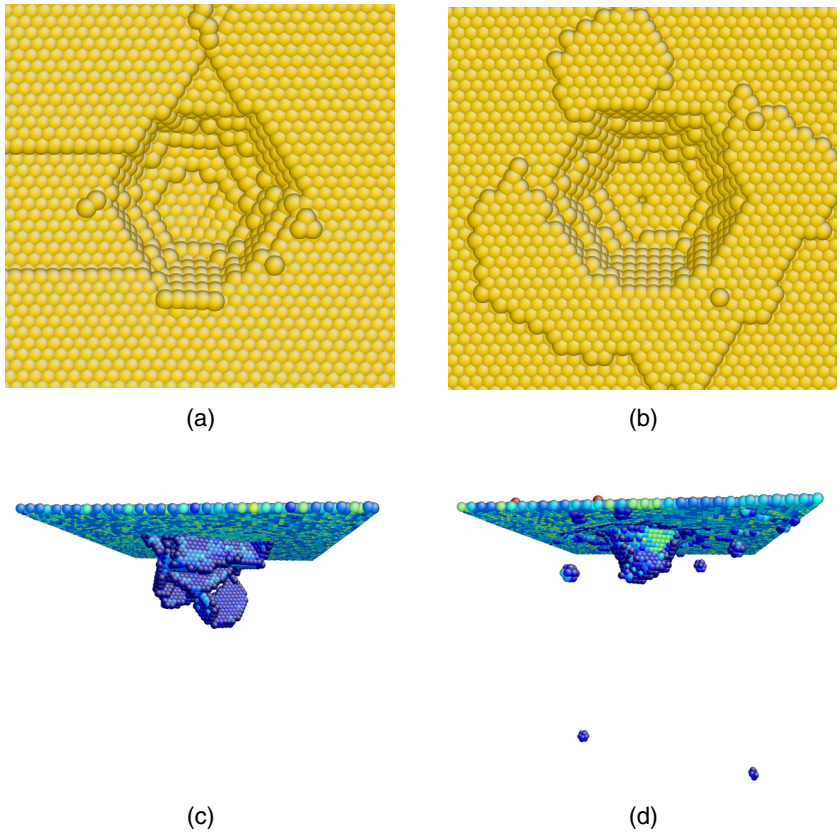

FIG. 2. Deformation mechanisms observed during nanoindentation are sensitive to temperature, indentation rate and indentation depth. Shown here are the surface profiles after indentations up to a depth of 15 Å performed using a spherically smooth indenter with $R = 20$ Å and an indentation rate of $\dot{h} = 80$ Å/ns. Simulations were performed at 20 K (2(a), 2(c)) and 1100 K (2(b), 2(d)). The surface profile at 20 K shows surface steps, ledges due to dislocation activity while the system at 1100 K contains ad-atom islands surrounding the indented region and this diffusive activity leads to extensive healing of the sheared regions of the sample resulting in a decrease in the dislocation density in the indented region as illustrated in Fig. 2(d). The formation of ad-atom island and the observation of significantly decreased dislocation density strongly suggests that diffusive processes are playing an important role. The atoms are colored using central symmetry coloring scheme in (c) and (d), hence atoms with fcc symmetry are not depicted. Structures from the high temperature simulations have been quenched to 10 K to remove the thermal fluctuations in the atomic positions.

An easy way to quantify the diffusive processes taking place in our indentation simulations is to study the evolution of the number of ad-atoms surrounding the indented region as a function of h at different temperatures. To this end, we assume a power-law relationship between the number of ad-atoms (N_a) and indentation depth, i.e. $N_a \propto h^{n_1}$. Using a least squares curve-fitting scheme, we obtain $n_1 \sim 1.50$ (see Fig. S3)[23] for simulations at 1000-1300 K, shallow depths ($h \sim$ 5-15 Å), an indentation rate of $\dot{h} = 5$ Å/ns, and using an indenter with tip radius $R = 20$ Å. For indentation simulations performed at temperatures below 700 K, we observe that dislocation activity becomes more pronounced and the value of the exponent increases. Similarly, upon increasing indentation depth to 25 Å, dislocation activity increases and the exponent n_1 increases to 2.23. These findings agree with the experimental results of Wang *et al.*[9] who reported an increase in activation volume from $0.4b^3$ to more than $20b^3$ in a single crystal of Cu with a tip radius of ~50 nm as the indentation depth was increased from 4.3 nm to 30 nm. This increase in n_1 suggests that with increase in the contact radius, the diffusive motion of atoms along the indenter-sample interface are unable to relieve the system of high stress and dislocation mediated processes becomes more dominant.

After investigating the microscopic processes at different indentation depths, we analyzed the sensitivity of the deformation mechanisms to the indentation rate. Fig. 3(a) shows the variation in the number of ad-atoms as a function of the indentation rate ($\dot{h}$) for fixed h at 1100 K. At

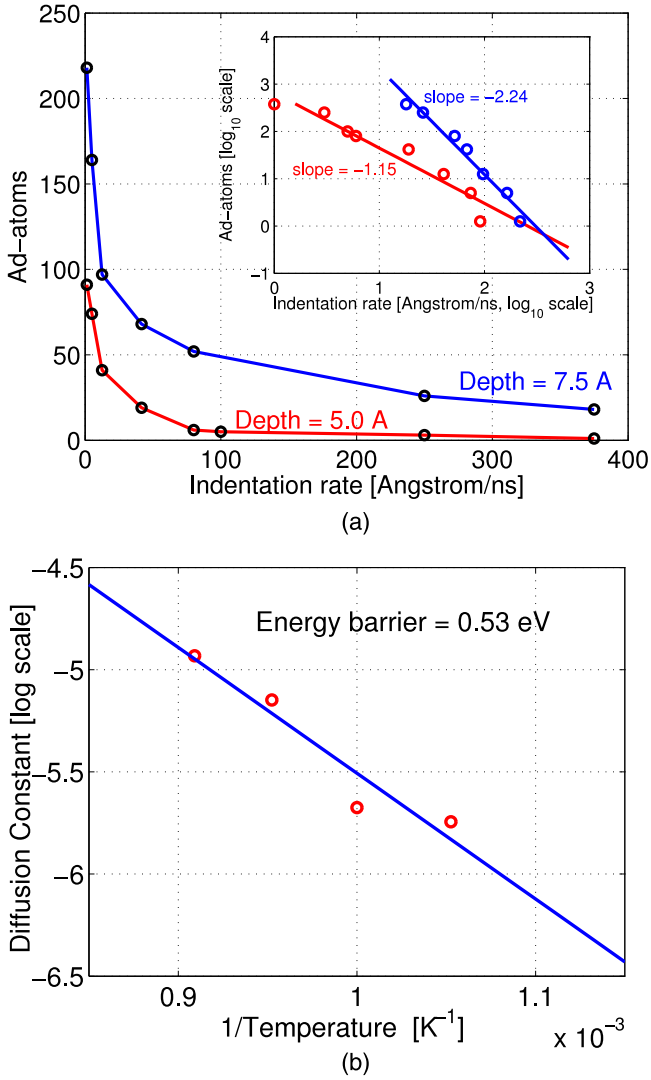

FIG. 3. 3(a) Analysis of the ad-atom island size at different indentation rates obtained from simulations at 1100 K using an indenter of radius 20 Å. At an indentation depth of $h = 5.0$ Å (red curve), the exponent n_2 is -1.15 (obtained from a least square fitting scheme using a log-log plot shown in the inset) while for $h = 7.5$ Å (blue curve) n_2 is -2.24. 3(b) Diffusion constant at different temperatures obtained from mean squared displacement analysis of structures obtained from MD simulations at 950 K, 1000 K, 1050 K and 1100 K for 5 ns. The diffusion barrier of 0.53 eV is close to the surface vacancy diffusion barrier in Cu.

slower indentation rates ($\dot{h} \sim 5$ Å/ns), the system has more time to generate defects that results in an increase in the ad-atom concentration. At very high indentation rates ($\dot{h} \sim$ 200-400 Å/ns), the formation and migration of ad-atoms is limited. At a fixed indentation depth of $h = 5$ Å, assuming that the indentation rate ($\dot{h}$) and the number of ad-atoms on the surface are related by a power-law relationship, $N_a \propto \dot{h}^{n_2}$, we find an exponent of $n_2 \sim -1.15$. When the indentation depth increases to $h = 7.5$ Å, we find that the exponent changes to $n_2 = -2.24$ most likely due to an increase in dislocation activity.

After analyzing how indentation depth and rate influence the deformation mechanisms, we turned our attention to how the system relaxes after a fixed-depth indentation event has occurred. To this end, we selected configurations from MD simulations at $h = 10$ Å and 20 Å and performed constant temperature runs (within the isothermal-isochoric ensemble) for 5 ns by keeping the indenter fixed. To gain insights into the probable atomic processes, we analyzed the structures by identifying atoms that moved more than nearest neighbor distance. This analysis suggests that surface

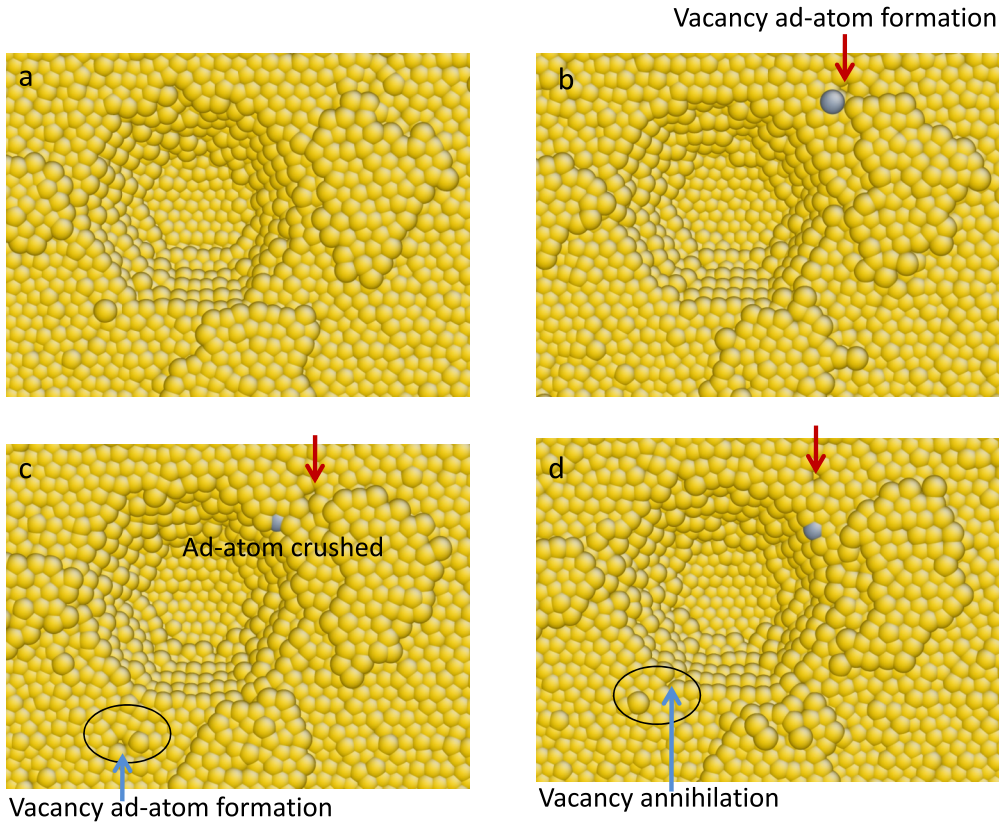

FIG. 4. By following the evolution of atoms on the indented surface at 1100 K, we observe unit atomic processes like vacancy ad-atom pair formation, ad-atom or vacancy annihilation, ad-atom and surface vacancy diffusion. The snapshots, separated by a time interval of 10 ps with respect to (a), show a surface vacancy ad-atom pair is formed in (b) (marked in blue) and the ad-atom is subsequently annihilated in (c). The vacancy, on the other hand, migrates to the indented region in about 50 ps. Another surface vacancy is formed in (c) and subsequently migrates to the indenter-sample interface in (d).

vacancy and ad-atom pair formation, ad-atom diffusion, surface vacancy diffusion, and clustering of ad-atoms occur in the vicinity of the indented region. A sequence of snapshots is shown in Fig. 4 where the formation of surface vacancy and ad-atom pairs close to the indented region can be seen. The free volume of surface vacancies was found to initially be localized around vacant lattice sites but eventually move toward the indented region and become delocalized. The majority of the ad-atoms were seen to form large clusters but a few were annihilated by surface vacancies.

A quantity that is often used to understand the dynamics of atoms is the root-mean-squared displacement (RMSD) profile:

$$r_{\mathrm{msd}}(t) = \frac{1}{6N}\sum_{i=1}^{N}\left[\mathbf{r}_i(t) - \mathbf{r}_i(0)\right]^2 \tag{1}$$

where, $\mathbf{r}_i(t)$ and $\mathbf{r}_i(0)$ are the position vectors of atom i at time t and $t = 0$, respectively and N represents the number of atoms. From the slopes of $r_{\mathrm{msd}}(t)$ vs t at different temperatures, we obtained an energy barrier of 1.43 eV and a diffusion pre-exponent of 1.421×10^3 Å^2/ps. As discussed in the supplementary materials (Table S1 and Fig. S4)[23] these values are close to the ad-atom and surface vacancy pair formation energy on Cu(111) surfaces.

Since, we now understand that the dynamics of ad-atoms leads to the formation of ad-atom islands on the surface, a question that remains unresolved is whether the surface vacancies are really able to migrate along the sample-indenter interface. To test this hypothesis, we calculated r_{msd} profiles at different temperatures for atoms only in the indented region. From the slopes of r_{msd} vs time at different temperatures (see Fig. 3(b)), we obtained an activation energy barrier of 0.53 eV

that is close to the surface vacancy diffusion barrier in Cu. This diffusion of vacancies is "short ranged" meaning that the vacancies involved are not diffusing from far off regions of the sample. Additionally, the diffusion barrier is smaller than the barrier needed to form surface vacancies which leads us to believe that this diffusional flow during nanoindentation is "source limited".

Our analysis of the high temperature indentation simulations and the results from d-AFED simulations at constant indentation depth clearly points to the possibility of a cross-over from a dislocation dominated plasticity to a diffusive mode of deformation depending on parameters like, temperature, indentation rate, indentation depth. Since, processes belonging to both these groups can be thermally activated and have different activation energies, there is an inherent time dependence in the response of the system to the indentation load. There is however, an interesting difference between the diffusive processes and displacive processes: while dislocation activity is generally delocalized (i.e. involves many atoms and has a higher activation volume),[11] diffusive processes are very localized. A direct consequence of this difference in activation volume is that displacive processes have a higher waiting time thus, resulting in lower strain rate and temperature susceptibility.

To further understand the reasons for the wide spectrum of strain rate exponents reported from experiments,[10,14,15] we analyzed the effect of indentation rate on stress relaxation and the diffusive processes. In nanoindentation experiments, the indentation rate is the speed with which the indenter tip moves normal to the surface of the sample. For typical indentation experiments the indenter velocity is $v_{\text{ind}} = \dot{h} \approx 10^{-9}$-$10^{-6}$ ms^{-1}. As the indenter penetrates the sample surface, the stress developed spreads over the whole material in the form of elastic waves whose velocity in an isotropic solid is $v_{\text{el}} = \sqrt{C_{11}/\rho} \approx 3.5 \times 10^3$ m/s for Cu, where C_{11} is the elastic modulus and ρ is the density. The high stress gradient imposed by the indenter can lead to dislocation nucleation or can activate diffusive processes like vacancy diffusion. The maximum velocity of these vacancies can be estimated from the chemical potential gradient. Using the indented sample, we obtain an estimate of the formation energy difference between a vacancy below the indenter tip and a vacancy placed just outside the indented region. In the elastically deformed sample (h ~4.20 Å) we find a chemical potential difference of ~0.50 eV. Thus, the velocity of vacancies (v_{vac}) migrating along the indenter/sample interface is

$$v_{\text{vac}} = \frac{\delta D_{\text{o}}}{\delta k_{\text{B}} T} e^{E_{\text{m}}/k_{\text{B}}T} \nabla \mu \tag{2}$$

where, δ is the interfacial layer thickness (≈ 5.0 Å), $\delta D_o = 5 \times 10^{-15}$ m^{3}s^{-1}, $E_m \approx 0.53$ eV obtained from our RMSD analysis and $\nabla\mu$ is the chemical potential gradient. Within this crude approximation, we obtain $v_{\text{vac}} \sim 10^{-6}$-$10^{-4}$ m/s at 300 K (most experiments are performed near room temperature conditions). Thus, for nanoindentation experiments (where $\dot{h} \sim 10^{-9}$ ms^{-1}), we find $v_{\text{el}} \gg v_{\text{vac}} \gg v_{\text{ind}}$ meaning that nanoindentation experiments are susceptible to diffusive mode of deformation and this can explain the low strain rate exponents and small activation volumes reported from experiments. On the other hand, for microindentation experiments $\dot{h} \sim 10^{-6}$ ms^{-1}, which means that $v_{\text{el}} \gg v_{\text{vac}} \sim v_{\text{ind}}$. Consequently, the deformation in microindentation is most probably dominated by dislocation activity, though diffusion can aid the initiation, multiplication or propagation of dislocations. Interestingly in computer simulations of indentation, the indentation rate is $\dot{h} \sim$ 1-100 m/s, which means that $v_{\text{vac}} \ll v_{\text{ind}}$ and thus, diffusive mode of deformation is clearly absent.

Indentation experiments performed by Klassen *et al.* on polycrystalline Cu samples at room temperature with an indentation rate of 0.05 μm/s suggest that $\hat{\Omega} \sim$ 240-1000b^3.[14] Such activation volumes correspond to dislocation activity in the bulk such as forest hardening, etc.[11] On the other hand, the slow indentation rates (about 1 nm/s) used by Schuh *et al.* and Cross *et al.* point to the existence of a diffusive regime and a small activation volume $\hat{\Omega} \sim 0.5b^3$.[2] This supports our conclusion that at higher indentation rates, deformation is dominated by dislocation activity.

We have shown that plastic deformation during indentation can be dominated by dislocation or diffusion activity. Experimental variables such as indentation rate, indenter tip radius, temperature and indentation depth are shown to govern these rate processes. We found that surface sources near the periphery of the indented region facilitate vacancy and ad-atom pair formation. Vacancies then

migrate along the indenter-sample interface to relieve system of the high compressive stress in the indented region. At slow indentation rates and/or high temperatures, the surface sources produce enough vacancies to accommodate the indenter. However, at low temperatures and high indentation rates, due to the lack of vacancies, dislocation activity becomes predominant.

ACKNOWLEDGMENTS

A. S. wishes to thank Andrew Lange and Ju Li for critical comments. This work was partially performed under the auspices of the U.S. Department of Energy by Lawrence Livermore National Laboratory under Contract DE-AC52-07NA27344. The work by A. S and W. E at Princeton was supported by the U. S. Department of Energy (DE-SC0009248) and by the Office of Naval Research (N00014-13-1-0338).

[1] S. G. Corcoran, R. J. Colton, E. T. Lilleodden, and W. W. Gerberich, Physical Review B **55**, 16057 (1997).
[2] C. A. Schuh, J. K. Mason, and A. C. Lund, Nature Materials **4**, 617 (2005).
[3] S. N. Dub, Y. Y. Lim, and M. M. Chaudhri, Journal of Applied Physics **107**, 043510 (2010).
[4] E. B. Tadmor, R. Miller, R. Phillips, and M. Ortiz, J. Mater. Res. **14**, 2233 (1999).
[5] A. Gouldstone, K. J. Van Vliet, and S. Suresh, Nature **411**, 656 (2001).
[6] K. J. Van Vliet, J. Li, T. Zhu, S. Yip, and S. Suresh, Physical Review B **67**, 104105 (2003).
[7] A. M. Minor, S. A. S. Asif, Z. W. Shan, E. A. Stach, E. Cyrankowski, T. J. Wyrobek, and O. L. Warren, Nature Materials **5**, 697 (2006).
[8] J. Li, K. J. Van Vliet, T. Zhu, S. Yip, and S. Suresh, Nature **418**, 307 (2002).
[9] F. Wang, P. Huang, and T. Lu, Journal of Materials Research **24**, 3277 (2009).
[10] J. K. Mason, A. C. Lund, and C. A. Schuh, Physical Review B **73**, 054102 (2006).
[11] T. Zhu, J. Li, A. Samanta, H. G. Kim, and S. Suresh, Proceedings of The National Academy of Sciences of The United States of America **104**, 3031 (2007).
[12] A. A. Elmustafa and D. S. Stone, Journal of The Mechanics And Physics of Solids **51**, 357 (2003).
[13] S. Saimoto, B. J. Diak, and K. R. Upadhyaya, Materials Science And Engineering A-Structural Materials Properties Microstructure And Processing **234**, 1015 (1997).
[14] R. J. Klassen, B. J. Diak, and S. Saimoto, Materials Science And Engineering A-Structural Materials Properties Microstructure And Processing **387**, 297 (2004).
[15] V. Bhakhri and R. J. Klassen, Scripta Materialia **55**, 395 (2006).
[16] T. Zhu, J. Li, A. Samanta, A. Leach, and K. Gall, Physical Review Letters **100**, 025502 (2008).
[17] A. Samanta, Ph.D. thesis, University of Pennsylvania, Philadelphia, USA, 2009.
[18] L. Maragliano and E. Vanden-Eijnden, Chemical Physics Letters **426**, 168 (2006).
[19] J. B. Abrams and M. E. Tuckerman, Journal of Physical Chemistry B **112**, 15742 (2008).
[20] T. Q. Yu, P. Y. Chen, M. Chen, A. Samanta, E. Vanden-Eijnden, and M. Tuckerman, The Journal of Chemical Physics **140**, 214109 (2014).
[21] A. Samanta, M. A. Morales, and E. Schwegler, The Journal of Chemical Physics **144**, 164101 (2016).
[22] P. J. Steinhardt, D. R. Nelson, and M. Ronchetti, Physical Review B **28**, 784 (1983).
[23] See supplementary material at http://dx.doi.org/10.1063/1.4958299 for simulation set up and the analyses of high temperature MD simulations and ad-atom vacancy pair formation barriers.
[24] J. A. Zimmerman, C. L. Kelchner, P. A. Klein, J. C. Hamilton, and S. M. Foiles, Physical Review Letters **87**, 165507 (2001).
[25] O. R. de la Fuente, J. A. Zimmerman, M. A. Gonzalez, J. de la Figuera, J. C. Hamilton, W. W. Pai, and J. M. Rojo, Physical Review Letters **88** (2002).
[26] H. Y. Liang, C. H. Woo, H. C. Huang, A. H. W. Ngan, and T. X. Yu, Philosophical Magazine **83**, 3609 (2003).
[27] S. J. Lloyd, A. Castellero, F. Giuliani, Y. Long, K. K. McLaughlin, J. M. Molina-Aldareguia, N. A. Stelmashenko, L. J. Vandeperre, and W. J. Clegg, Proceedings of The Royal Society A-Mathematical Physical And Engineering Sciences **461**, 2521 (2005).